Correspondence

Interpolation-Dependent Image Downsampling

Yongbing Zhang, Debin Zhao, Jian Zhang, Ruiqin Xiong, and Wen Gao, *Fellow, IEEE*

***Abstract*—Traditional methods for image downsampling commit to remove the aliasing artifacts. However, the influences on the quality of the image interpolated from the downsampled one are usually neglected. To tackle this problem, in this paper, we propose an interpolation-dependent image downsampling (IDID), where interpolation is hinged to downsampling. Given an interpolation method, the goal of IDID is to obtain a downsampled image that minimizes the sum of square errors between the input image and the one interpolated from the corresponding downsampled image. Utilizing a least squares algorithm, the solution of IDID is derived as the inverse operator of upsampling. We also devise a content-dependent IDID for the interpolation methods with varying interpolation coefficients. Numerous experimental results demonstrate the viability and efficiency of the proposed IDID.**

***Index Terms*—Downsampling, interpolation, least squares, upsampling.**

I. Introduction

Accelerated development in electronic technology and computer hardware brought about substantive increase in display devices offering a wide range of image resolutions (e.g., computer monitors, laptop computer screens, personal digital assistants, and cell phones). To convert images with different resolutions between devices with different display sizes, it is desirable to develop efficient image downsampling and upsampling (interpolation) techniques. Image downsampling is a process to make a digital image smaller by removing pixels. By contrast, interpolation is a process to make a digital image larger by interpolating pixels. Both image downsampling and interpolation have wide applications in image/video processing. In addition to the conversion between different image sizes, downsampling and interpolation are alternative approaches to achieve better performance for low-bit-rate image coding [1]–[3], where images are downsampled prior to compression, and then, the missing portions are interpolated after decompression. Image downsampling can be also utilized in SD/HD video coding, where an HD sequence is downsampled to SD before encoding, and then, the decoded SD sequence can be used for an SD-display device or converted to HD via interpolation for an HD-display device. In addition, image downsampling and interpolation are important techniques for spatial scalable video coding [4].

Image downsampling is usually manipulated in spatial or frequency domains. In the spatial domain, downsampling can be performed by uniformly retaining the corresponding pixels within the input image. It is also referred to as direct downsampling, which is the easiest downsampling algorithm. However, aliasing artifacts can be observed in the direct downsampled image due to the overlapping of downsampled spectra. To alleviate the aliasing artifacts, filtering is usually performed prior to direct downsampling to limit the bandwidth of the input image. In [1], an analytical model for JPEG encoders was derived to obtain an optimality criterion on the downsampling factor for a given input image. In [5], the downsampled image was obtained by directional prefiltering and uniform downsampling. In the frequency domain, wavelet transforms [6], and discrete cosine transforms (DCTs) [7], [8] are usually employed for image downsampling, where the transformed coefficients of low frequencies are maintained, whereas other coefficients are discarded. Jung *et al.* in [9] introduced "subband DCT," which was later used for image resizing in the compressed domain [10].

Various interpolation techniques have been suggested for improving the quality of a high-resolution image. Popular interpolation methods, which are commonly used in image/video software and hardware products, are bilinear interpolation, cubic convolution interpolation [9], and cubic spline interpolation [10]. Such methods gain their popularity mainly due to their relatively low complexity. However, these interpolation methods fail to capture the fast-evolving statistics around edges and consequently produce images with jaggies, blurring, and ringing artifacts. Actually, it is a challenge to best preserve the sharpness of edges in image interpolation. To address this problem, several edge-guided methods [11]–[14] have been recently proposed. Wang and Ward [11] proposed to derive the edge direction by making use of gradients and get the best correlation pixels with the pixel to be interpolated. In [12], two interpolation results were fused in two mutually orthogonal directions using the statistics of a local window. In [13], Li and Orchard proposed an edge-directed interpolation (EDI) utilizing the covariance of a low-resolution image to estimate the high-resolution-image covariance, which represents the edge direction information to some extent. In our previous work [14], a nonlocal EDI (NLEDI) was proposed by further taking the advantage of a nonlocal-means filter [15].

Nowadays, there appear more and more interpolation methods with superior performance. However, few joint downsampling and interpolation algorithms are studied in the literature. In [2] and [16], the optimal interpolations were studied given the downsampling filter. Variable projection was utilized in [2] to devise the optimal interpolation coefficients given the downsampling filters, and they also explored the use of optimal downsampling and interpolation filters for low bit-rate image coding. In [16], a technique was proposed to identify patterns associated with different downsampling methods so as to select the appropriate interpolation mechanism. In [17] and [18], Goutsias and Heijmans proposed a *pyramid condition* that the downsampling operator after upsampling should give the identity operator. However, as stated in [17] and [18] the upsampling operator, after downsampling, usually cannot result in the identity operator. Therefore, the difference

Manuscript received June 07, 2010; revised October 19, 2010, December 20, 2010, and March 08, 2011; accepted May 17, 2011. Date of publication May 31, 2011; date of current version October 19, 2011. This work was supported in part by the National Science Foundations of China under Grant 60736043 and Grant 61073083 and in part by the Major State Basic Research Development Program of China (973 Program) under Grant 2009CB320905. The Associate Editor coordinating the review of this manuscript and approving it for publication is Prof. Rafael Molina.

Y. Zhang was with the Department of Computer Science, Harbin Institute of Technology, Harbin 150001, China. He is now with the Graduate School at Shenzhen, Tsinghua University, Shenzhen 518055, China (e-mail: ybzhang@mail.tsinghua.edu.cn).

D. Zhao and J. Zhang are with the Department of Computer Science, Harbin Institute of Technology, Harbin 150001, China (e-mail: dbzhao@vilab.hit.edu.cn; zhangjian@jdl.ac.cn).

R. Xiong and W. Gao are with the National Engineering Laboratory for Video Technology, Key Lab of Machine Perception, School of Electronics Engineering and Computer Sciences, Peking University, Beijing 100871, China (e-mail: rqxiong@pku.edu.cn; wgao@pku.edu.cn).

Color versions of one or more of the figures in this paper are available online at http://ieeexplore.ieee.org.

Digital Object Identifier 10.1109/TIP.2011.2158226

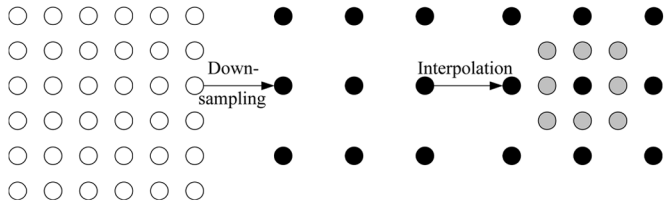

Fig. 1. Image downsampling and interpolation.

between the input signal and the one generated by the upsampling operator, which is termed as the *detail signal* in [17] and [18], is indispensable for perfect reconstruction. It would be desirable to minimize the energy of the *detail signal*. However, [17] and [18] did not give a solution to tackle this problem.

In this paper, an interpolation-dependent image downsampling (IDID) is proposed, where the difference between the input image and the one generated by a specific interpolation method is minimized. Part of our previous work has been published in [19]. Different from traditional image downsamplings, which usually neglect the influence on the quality of upsampled image interpolating from the downsampled one, interpolation is hinged to downsampling in the proposed IDID. In particular, for each pixel $X(i,j)$ to be downsampled, all its neighboring pixels involving $X(i,j)$ during interpolation are identified. The optimal downsampled value of $X(i,j)$ is the one that minimizes the sum of square errors between the original and interpolated intensity values within all the identified neighboring pixels. A content-dependent IDID is also devised for the interpolation methods with varying interpolation coefficients.

The remainder of this paper is organized as follows: Section II gives a detailed description of the proposed IDID. Section III elaborates a content-dependent IDID for those interpolations with varying coefficients. In Section IV, experimental results are provided. Finally, this paper is summarized in Section V.

II. Problem Formulation

Most existing interpolation methods attempt to exploit the information of a low-resolution image to generate a high-resolution one with much better visual quality. Aside from the performance of the interpolation method, image downsampling also plays a critical role for the quality of the interpolated image. This is because downsampling an image may give rise to the loss of image information that cannot be recovered by interpolation. For a given interpolation method, the more information the low-resolution image contains, the better visual quality the interpolated high-resolution image will exhibit. Consequently, in order to obtain a higher quality interpolated image, it is desirable to maintain more information during image downsampling.

Fig. 1 gives the sketch map of the image downsampling and interpolation process, where the white circles indicate the original pixels located within the input image, the black circles the downsampled pixels, and the gray circles the interpolated pixels during the interpolation process. Let $\mathbf{Y}$ denote the input image of size $M\times N$, $\mathbf{X}$ the image after downsampling to size $M/2\times N/2$, and $\hat{\mathbf{Y}}$ the upsampled image after interpolation. The goal of the proposed IDID is to obtain an optimal downsampled image that enables the upsampled image to have the highest quality. Consequently, the optimal downsampled image should satisfy

$$\mathbf{X}=\arg\min_{\mathbf{X}}\|\hat{\mathbf{Y}}-\mathbf{Y}\|^2 \tag{1}$$

where $\mathbf{X}=[X_{0,0},X_{0,1},\ldots,X_{0,N/2-1},X_{1,0},X_{1,1},\ldots,X_{1,N/2-1},\ldots,X_{M/2-1,0},X_{M/2-1,1},\ldots,X_{M/2-1,N/2-1}]^T$ and $\mathbf{Y}=[Y_{0,0},Y_{0,1},\ldots,Y_{0,N-1},Y_{1,0},Y_{1,1},\ldots,Y_{1,N-1},\ldots,Y_{M-1,0},Y_{M-1,1},\ldots,Y_{M-1,N-1}]^T$.

Obviously, (1) indicates that the proposed downsampling method depends on the interpolation process. For each downsampled pixel $X(i,j)$, shown as the center of the nine black circles in Fig. 1, all its neighboring pixels involving $X(i,j)$ during interpolation are identified as the gray circles in Fig. 1. The optimization target of the proposed IDID is to minimize the sum of square errors among all the identified pixels and the corresponding original ones. It is noted that, in Fig. 1, we assume that the value of each interpolated pixel only depends on its four closest pixels, and it can be easily extended to an arbitrary number of closest pixels.

Given the input image $\mathbf{X}$, the interpolation process can be expressed as

$$\hat{\mathbf{Y}}=\mathbf{H}\mathbf{X} \tag{2}$$

where $\mathbf{H}$ represents the interpolation matrix. It is noted that $\mathbf{H}$, which is composed of coefficients of a specific interpolation method, can be specified as

$$\mathbf{H}=\begin{bmatrix} h_{0,0} & h_{0,1} & \cdots & h_{0,M/2\times N/2-1} \\ h_{1,0} & h_{1,1} & \cdots & h_{1,M/2\times N/2-1} \\ h_{2,0} & h_{2,1} & \cdots & h_{2,M/2\times N/2-1} \\ \cdots & \cdots & \cdots & \cdots \\ h_{M\times N-1,0} & h_{M\times N-1,1} & \cdots & h_{M\times N-1,M/2\times N/2-1} \end{bmatrix} \tag{3}$$

where $h_{k,l}$ represents the interpolation coefficient contributed by the lth downsampled pixel during interpolation of the kth pixel. Here, both the interpolated and downsampled pixels are represented in a concatenated and lexicographical order. Incorporating (3) and (2) into (1), the objective function to derive the optimal downsampled image can be expressed as

$$J=\min_{\mathbf{X}}\|\mathbf{H}\mathbf{X}-\mathbf{Y}\|^2. \tag{4}$$

Setting the partial derivative of J to be zero, we derive

$$\frac{\partial J}{\partial \mathbf{X}}=2\mathbf{H}^T(\mathbf{H}\mathbf{X}-\mathbf{Y})=0. \tag{5}$$

The optimal downsampled image can be then expressed as

$$\mathbf{X}^*=(\mathbf{H}^T\mathbf{H})^{-1}\mathbf{H}^T\mathbf{Y}. \tag{6}$$

Obviously, the proposed downsampling operator is the left-inverse operator for a full-rank interpolation operator. It should be noted that the pyramid condition [17], [18] leads to the same downsampling operator as the proposed IDID. However, [17] and [18] did not give a closed-form solution of optimal downsampling operator for a given interpolation operator.

III. Content-Dependent IDID

It is noted that, in (6), the interpolation matrix $\mathbf{H}$ must be available before downsampling. For those content-independent interpolation methods, IDID can be directly performed utilizing the available interpolation matrix. However, for the content-dependent interpolation methods, interpolation matrix $\mathbf{H}$ is not available before downsampling. Consequently, (6) cannot be directly utilized. To tackle such a problem, we propose a content-dependent IDID, which is summarized in Table I.

TABLE I
SUMMARY OF THE PROPOSED CONTENT-DEPENDENT IDID

initialize $\mathbf{H}^0$ and $\mathbf{X}^0$
for $i = 1$ to iMax-1
Compute $\mathbf{H}^i$ based on $\mathbf{X}^{i-1}$, *e.g.* according to Eq. (3) and the content-dependent interpolation matrix derivation method.
Compute $\mathbf{X}^i$ according to Eq. (6)
Compute the MSE: $E(i)=\frac{4}{MN}\left\|\mathbf{X}^i-\mathbf{X}^{i-1}\right\|^2$
if $E(i)<T$
break
end if
end for

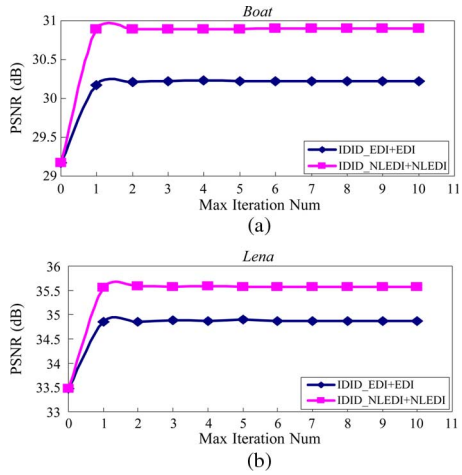

Fig. 2. PSNR values of interpolated image by the content-dependent IDID versus iteration number.

In the initialization stage, initial values $\mathbf{H}^0$ and $\mathbf{X}^0$ are first set. In this paper, $\mathbf{H}^0$ is comprised of bilinear interpolation coefficients, and $\mathbf{X}^0$ is set to be the result generated by the direct downsampling. During each iteration, we first update $\mathbf{H}^i$ according to the previous value of $\mathbf{X}^{i-1}$, and then, we obtain $\mathbf{X}^i$ based on the updated $\mathbf{H}^i$ according to (6). Subsequently, we compute the difference between $\mathbf{X}^i$ and $\mathbf{X}^{i-1}$. If the difference is below a given threshold T, it is considered that the content-dependent IDID has converged, and the iteration can be terminated. Otherwise, the algorithm moves to the next iteration. In this paper, threshold T is set to be 0.5.

The peak signal-to-noise ratio (PSNR) values of interpolated images versus the iteration number of the proposed content-dependent IDID are illustrated in Fig. 2. Here, IDID_EDI + EDI represent that the input image is first downsampled by IDID, where the interpolation matrix is composed of EDI coefficients, and then, the downsampled image is interpolated by EDI. Similarly, IDID_NLEDI + NLEDI represent that the input image is first downsampled by IDID, where the interpolation matrix is composed of NLEDI coefficients, and then, the downsampled image is interpolated by NLEDI. Different from EDI, NLEDI assigns each pixel sample a unique weight value according to the structure similarity, compared with that of the center sample. Consequently, it achieves better performance than EDI for the majority cases; see [14] for more details.

It is shown that, compared with the direct downsampling method (when iteration number is 0), IDID_EDI and IDID_NLEDI are able to obtain downsampled images from which interpolated images with much higher PSNR values can be generated. Another observation is that the PSNR values of the interpolated images tend to be converged when the iteration number exceeds 2, e.g., there is very little fluctuation among the interpolated images when the iteration number is larger than 2, which reflects the stability of IDID. Based on the observation in Fig. 2, the iteration number is set to be 2 for content-dependent IDID in this paper.

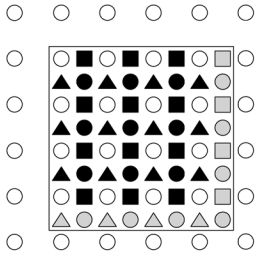

Fig. 3. Blockwise implementation of IDID.

IV. EXPERIMENTAL RESULTS

To evaluate the proposed IDID, extensive experiments were carried out in this section. First a blockwise implementation of IDID is provided to reduce the storage and computational complexities. Then, the downsampling and interpolation comparisons are presented. Finally, an IDID-based low-bit-rate image compression scheme is given in the third subsection.

A. Blockwise Implementation

It is noted that the dimension of matrix $\mathbf{H}$ in (6) is $(MN) \times (MN/4)$, which is too demanding in terms of storage and computational complexities. To tackle this problem, a blockwise IDID is proposed and will be used in the following experiments. The downsampling and interpolation process of the blockwise implementation is depicted in Fig. 3, where the white dots represent the downsampled pixels, the black dots the interpolated pixels along the diagonal direction, the square dots the interpolated pixels along the horizontal direction, and the triangle dots the interpolated pixels along the vertical direction. All the dots surrounded by the solid line belong to the same block. It is noted that the interpolation of boundary pixels will involve the downsampled pixels outside the current block, e.g., the interpolations of the pixels indicated by the gray circles, gray squares, and gray triangles in Fig. 3 involve the downsampled pixels outside the current block.

To tackle such a problem, the interpolation of $\hat{\mathbf{Y}}$ can be reformulated as

$$\hat{\mathbf{Y}} = \mathbf{H}\mathbf{X} + \mathbf{\Phi} \tag{7}$$

where $\mathbf{\Phi}$ is a column vector representing the contribution of downsampled pixels outside the current block. For the pixel, whose interpolation does not involve those downsampled pixels outside the current block, the corresponding element of $\mathbf{\Phi}$ is set to be zero. In addition, for the pixel, whose interpolation involves those downsampled pixels outside the current block, the corresponding element of $\mathbf{\Phi}$ is the summation of multiplication between the interpolation coefficients and the corresponding pixels outside the current block. In the experiment, the block size of IDID is set to be 16.

B. Downsampling and Interpolation Comparisons

Seven sample images varying in size and content are selected in this subsection to demonstrate the superior information preserving ability of IDID. These test images include: *Boat* (512 × 512), *Lena* (512 × 512), *Elaine* (512 × 512), *Couple* (512 × 512), *Cap* (768 × 512),

TABLE II
PSNR (IN DECIBELS) COMPARISON OF DIFFERENT COMBINATIONS OF DOWNSAMPLING AND INTERPOLATION

Image	Method	Bilinear	Bicubic	EDI	NLEDI
Boat	Direct	29.169	29.271	29.194	29.529
	MPEG-B	28.880	29.399	28.964	29.222
	IDID_Bilinear	**30.285**	30.580	29.919	30.483
	IDID_Bicubic	30.175	**30.726**	29.914	30.463
	IDID_EDI	29.722	29.889	**30.441**	30.510
	IDID_NLEDI	29.901	30.153	30.251	**30.894**
Lena	Direct	33.472	34.013	33.925	34.335
	MPEG-B	32.822	33.621	33.188	33.483
	IDID_Bilinear	**34.480**	34.976	34.037	34.602
	IDID_Bicubic	34.289	**35.226**	34.215	34.785
	IDID_EDI	33.852	34.401	**35.077**	35.230
	IDID_NLEDI	33.953	34.589	34.904	**35.533**
Elaine	Direct	31.814	31.541	32.020	32.115
	MPEG-B	32.551	32.879	32.711	32.792
	IDID_Bilinear	**33.265**	33.328	33.018	33.177
	IDID_Bicubic	33.175	**33.435**	33.093	33.242
	IDID_EDI	32.990	33.104	**33.288**	33.336
	IDID_NLEDI	33.045	33.178	33.250	**33.402**
Couple	Direct	26.598	26.565	26.355	26.449
	MPEG-B	26.810	27.137	26.748	26.981
	IDID_Bilinear	**27.679**	27.850	27.334	27.605
	IDID_Bicubic	27.636	**27.932**	27.316	27.614
	IDID_EDI	27.308	27.388	**27.371**	27.373
	IDID_NLEDI	27.399	27.525	27.275	**27.606**
Cap	Direct	33.367	33.447	33.677	34.013
	MPEG-B	32.646	33.079	32.875	33.020
	IDID_Bilinear	**34.099**	34.341	34.097	34.633
	IDID_Bicubic	33.999	**34.465**	34.063	34.575
	IDID_EDI	33.566	33.720	**34.741**	34.812
	IDID_NLEDI	33.718	33.898	34.606	**35.118**
Motor	Direct	25.650	25.896	25.923	26.351
	MPEG-B	24.669	25.171	24.895	25.149
	IDID_Bilinear	**26.252**	26.606	26.096	26.712
	IDID_Bicubic	26.147	**26.740**	26.106	26.719
	IDID_EDI	25.675	25.894	**26.891**	27.046
	IDID_NLEDI	25.802	26.095	26.694	**27.397**
Parrot	Direct	34.450	34.983	35.127	35.737
	MPEG-B	33.289	33.946	33.678	33.969
	IDID_Bilinear	**35.098**	35.619	34.922	35.690
	IDID_Bicubic	34.963	**35.804**	35.057	35.806
	IDID_EDI	34.460	34.946	**36.038**	36.181
	IDID_NLEDI	34.582	35.162	35.726	**36.629**

Parrot (768 × 512), and *Motor* (768 × 512). Each image is downsampled to one fourth of the original sizes (i.e., each dimension is divided in half) and then interpolated to the original resolution. Bilinear, Bicubic, EDI, and NLEDI are utilized for interpolation in the experiment.

The following six methods are used for downsampling.

1) Direct-subsampling: The downsampled value is the upper left one of the four corresponding intensity values.
2) MPEG-B downsampling: Each image is first filtered to reduce the bandwidth and then downsampled by the direct-subsampling method. The filter coefficient is set to be [2, 0, −4, −3, 5, 19, 26, 19, 5, −3, −4, 0, 2]/64 [20].
3) IDID_Bilinear: Each image is downsampled by IDID, where the interpolation matrix is composed of Bilinear interpolation coefficients.
4) IDID_Bicubic: Each image is downsampled by IDID, where the interpolation matrix is composed of Bicubic interpolation coefficients.
5) IDID_EDI: Each image is downsampled by IDID, where the interpolation matrix is composed of EDI coefficients.
6) IDID_NLEDI: Each image is downsampled by IDID, where the interpolation matrix is composed of NLEDI coefficients.

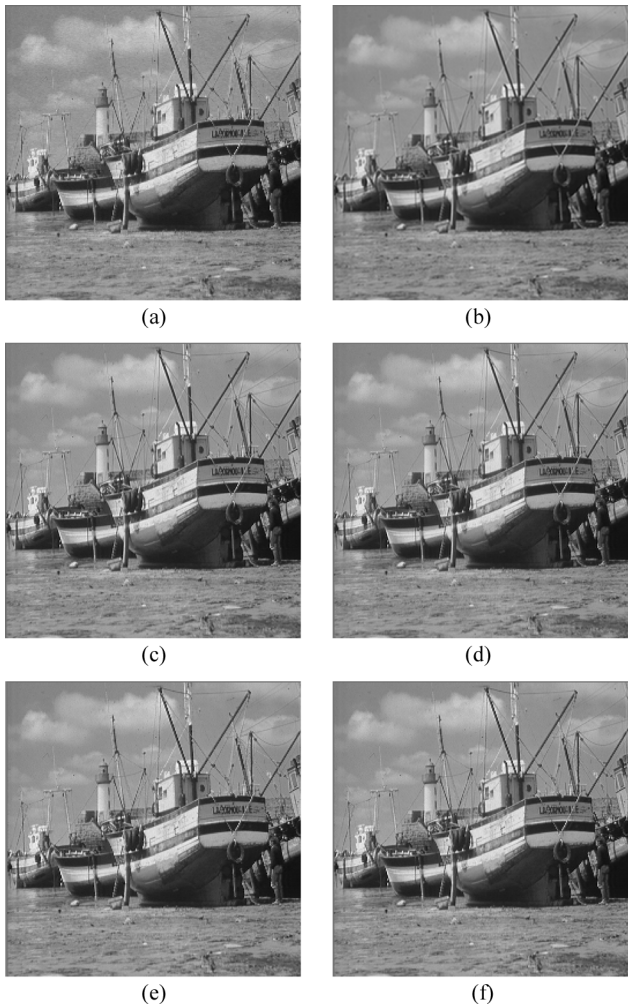

Fig. 4. Different downsampled versions of Boat. (a) Direct subsampling. (b) MPEG-B downsampling. (c) IDID_Bilinear. (d) IDID_Bicubic. (e) IDID_EDI. (f) IDID_NLEDI.

The PSNR comparisons among different combinations of downsampling and interpolation methods are illustrated in Table II, where the methods in the second column are downsampling methods and the methods in the first row are interpolation methods. Three findings have been observed from the experiments. First, the downsampling methods have a significant quantitative effect on the interpolated images. For the majority images, the differences between the best and worst interpolation and downsampling combinations are more than 1 dB. From the downsampled images generated by the direct downsampling and MPEG-B downsampling, the interpolated images with the lowest PSNR are obtained for almost all the interpolation methods over each test image. This is due to the fact that these two downsampling algorithms neglect the effect of interpolation. Second, IDID is able to preserve more image information than the direct and MPEG-B downsampling algorithms do. Almost for all the test images, the interpolated images generated from the downsampled ones by IDID are of higher PSNR, compared with those generated from the downsampled ones by direct and MPEG-B downsampling methods. This is because much more detailed information that is necessary for interpolation is absorbed in IDID. Third, for each interpolation method, IDID whose interpolation matrix is composed of the coefficients of the corresponding interpolation method achieves the highest PSNR. For example, Bilinear interpolation exhibits the

TABLE III
PSNR COMPARISONS OF DIFFERENT COMPRESSION METHODS UNDER VARIOUS BITS PER PIXEL

Image	Rate (bpp)	Methods								
		JPEG	Direct downsampling				IDID_Bilinear	IDID_Bicubic	IDID_EDI	IDID_NLEDI
			Bilinear	Bicubic	EDI	NLEDI	Bilinear	Bicubic	EDI	NLEDI
Boat	0.20	26.254	27.021	26.965	26.938	27.131	27.507	27.503	27.353	27.616
	0.25	27.531	27.524	27.486	27.459	27.684	28.023	28.175	27.906	28.303
	0.30	28.478	27.864	27.839	27.800	28.064	28.550	28.649	28.435	28.794
Elaine	0.15	28.076	30.248	30.151	30.309	30.367	30.506	30.570	30.515	30.581
	0.20	29.606	30.624	30.558	30.706	30.763	31.174	31.136	31.185	31.262
	0.25	30.665	30.815	30.653	30.898	30.968	31.529	31.629	31.631	31.716

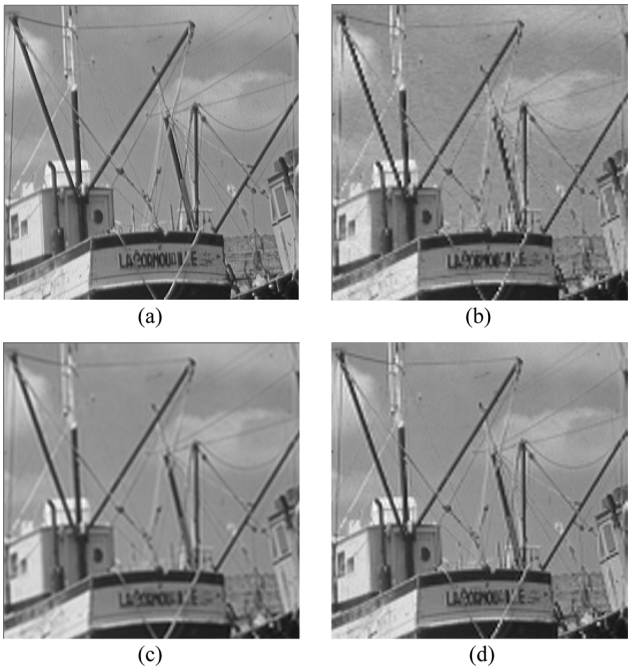

Fig. 5. Upper-right-quarter comparisons among different interpolation versions of Boat. (a) Original image. (b) Interpolated image generated by the combination of direct downsampling and Bicubic interpolation. (c) Interpolated image generated by the combination of MPEG-B downsampling and Bicubic interpolation. (d) Interpolated image generated by the combination of IDID_Bicubic downsampling and Bicubic interpolation.

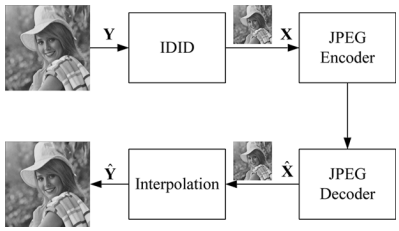

Fig. 6. IDID-based low-bit-rate image compression.

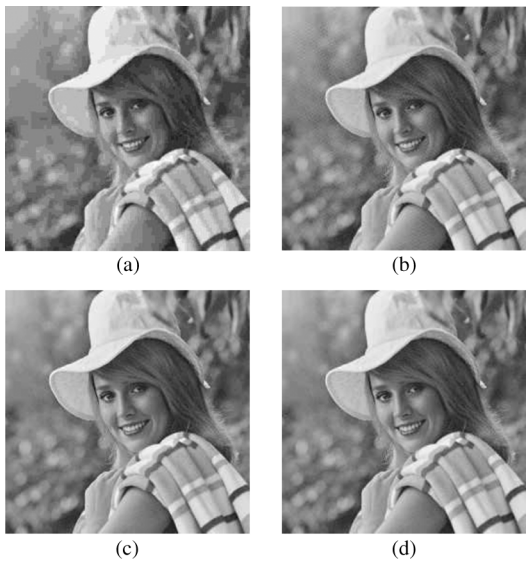

Fig. 7. Visual comparisons among different compression methods at 0.20 bpp for Elaine (512 × 512). (a) JPEG (0.21 bpp; 29.939 dB). (b) Direct + NLEDI (0.21 bpp; 30.858 dB). (c) IDID_Bilinear + Bilinear (0.20 bpp; 31.174 dB). (d) IDID_NLEDI + NLEDI (0.20 bpp; 31.262 dB).

best performance when IDID_Bilinear is applied. Similarly, Bicubic, EDI, and NLEDI have the best performance when the corresponding IDID_Bicubic, IDID_EDI, and IDID_NLEDI are applied, shown as the PSNR values represented in bold type in Table II. This further verifies that IDID is an optimal downsampling operator for a specific interpolation algorithm.

As an example, Fig. 4 depicts the different downsampled versions of Boat generated by various methods. Obviously, the downsampled images generated by IDID are able to not only improve the quality of interpolated images but also exhibit quite good visual quality.

The upper-right-quarter comparisons among interpolated images of Boat, generated by different combinations of downsampling and Bicubic interpolation, are provided in Fig. 5. It is noted that all the interpolated images are generated by Bicubic. Obviously, the interpolated image generated from the direct downsampled version exhibits serious sawtooth artifacts along mast regions. In addition, strong blurring artifacts exhibit in the interpolated image generated from the MPEG-B downsampled version. On the contrary, fewer sawtooth and blurring artifacts can be observed in the interpolated image generated from the IDID_Bicubic downsampled version.

C. Low-Bit-Rate Image Compression

Here, an IDID-based low-bit-rate image compression is presented. As shown in Fig. 6, the presented low-bit-rate image compression is composed of four components: 1) IDID; 2) JPEG encoder; 3) JPEG decoder; and 4) interpolation.

Elaine (512 × 512) and Boat (512 × 512) are selected to test the efficiency of the proposed IDID-based low-bit-rate image compression. The PSNR results of different methods are listed in Table III, where the methods in the second row are downsampling methods and the methods in the third row are interpolation methods. It is noted that IDID_Bilinear represents that the interpolation matrix of IDID is composed of coefficients of Bilinear. Similarly, IDID_Bicubic, IDID_EDI, and IDID_NLEDI represent that the interpolation matrix of IDID is composed of coefficients of Bicubic, EDI, and NLEDI, respectively. The results are tabulated against the bit rates from 0.15 to 0.25 bpp.

In most cases, the direct downsampling method outperforms JPEG, without downsampling. This is because only a quarter of the original data is needed to compress in the downsampling compression scenario. The IDID-based image compression scheme significantly outperforms the former two. This can be attributed to the property that IDID is able to preserve more information in the downsampled images.

Fig. 7 gives the visual comparisons among different compression methods at 0.20 bpp for Elaine (512×512). It is shown that JPEG results in the worst visual quality due to the existence of severe blocking artifacts. In the reconstructed image by Direct + NLEDI (direct downsampling and NLEDI interpolation), blocking artifacts disappeared; however, there is much more noise. This is because a lot of detail information is lost during direct downsampling, and it cannot be recovered by NLEDI. On the contrary, the reconstructed images by IDID_Bilinear + Bilinear (IDID_Bilinear downsampling and Bilinear interpolation) and IDID_NLEDI + NLEDI (IDID_NLEDI downsampling and NLEDI interpolation) exhibit better visual quality and higher PSNR.

V. Conclusion

An IDID algorithm has been proposed in this paper. Different from other downsampling algorithms, the proposed IDID hinges the interpolation to the downsampling process. For each input image, the IDID is able to obtain an optimal downsampled image from which a high-visual-quality image with the same resolution as the input image is generated. We have also proposed a content-dependent IDID algorithm for the interpolation methods with varying interpolation coefficients. Experimental results demonstrate the viability and efficiency of the proposed IDID.

References

[1] A. M. Bruckstein, M. Elad, and R. Kimmel, "Down scaling for better transform compression," *IEEE Trans. Image Process.*, vol. 12, no. 9, pp. 1132–1144, Sep. 2003.

[2] Y. Tsaig, M. Elad, P. Milanfar, and G. H. Golub, "Variable projection for near-optimal filtering in low bit-rate block coders," *IEEE Trans. Circuits Syst. Video Technol.*, vol. 15, no. 1, pp. 154–160, Jan. 2005.

[3] W. Lin and D. Li, "Adaptive downsampling to improve image compression at low bit rates," *IEEE Trans. Image Process.*, vol. 15, no. 9, pp. 2513–2521, Sep. 2006.

[4] H. Schwarz, D. Marpe, and T. Wiegand, "Overview of the scalable video coding extension of the H.264/AVC standard," *IEEE Trans. Circuits Syst. Video Technol.*, vol. 17, no. 9, pp. 1103–1120, Sep. 2007.

[5] X. Wu, X. Zhang, and X. Wang, "Low bit-rate image compression via adaptive down-sampling and constrained least squares upconversion," *IEEE Trans. Image Process.*, vol. 18, no. 3, pp. 552–561, Mar. 2009.

[6] M. Vetterli and J. Kovacevic, *Wavelets and Subband Coding*. Englewood Cliffs, NJ: Prentice-Hall, 1995.

[7] S. H. Jung, S. K. Mitra, and D. Mukherjee, "Subband DCT: Definition, analysis, and applications," *IEEE Trans. Circuits Syst. Video Technol.*, vol. 6, no. 3, pp. 273–286, Jun. 1996.

[8] D. Mukherjee and S. K. Mitra, "Image resizing in the compressed domain using subband DCT," *IEEE Trans. Circuits Syst. Video Technol.*, vol. 12, no. 7, pp. 620–627, Jul. 2002.

[9] R. G. Keys, "Cubic convolution interpolation for digital image processing," *IEEE Trans. Acoust., Speech, Signal Process.*, vol. ASSP-29, no. 6, pp. 1153–1160, Dec. 1981.

[10] H. S. Hou and H. C. Andrews, "Cubic splines for image interpolation and digital filtering," *IEEE Trans. Acoust., Speech, Signal Process.*, vol. ASSP-26, no. 6, pp. 508–517, Dec. 1978.

[11] Q. Wang and R. Ward, "A new orientation-adaptive interpolation method," *IEEE Trans. Image Process.*, vol. 16, no. 4, pp. 889–900, Apr. 2007.

[12] L. Zhang and X. Wu, "An edge-guided image interpolation algorithm via directional filtering and data fusion," *IEEE Trans. Image Process.*, vol. 15, no. 8, pp. 2226–2238, Aug. 2006.

[13] X. Li and M. T. Orchard, "New edge-directed interpolation," *IEEE Trans. Image Process.*, vol. 10, no. 10, pp. 1521–1527, Oct. 2001.

[14] X. Zhang, S. Ma, Y. Zhang, L. Zhang, and W. Gao, "Nonlocal edge-directed interpolation," in *Proc. IEEE Pacific-Rim Conf. Multimedia*, Dec. 2009, pp. 1197–1207.

[15] A. Buades, B. Coll, and J. M. Morel, "A non-local algorithm for image denoising," in *Proc. IEEE Int. Conf. Comput. Vis. Pattern Recog.*, Jun. 2005, pp. 60–65.

[16] T. Frajka and K. Zeger, "Downsampling dependent upsampling of images," *Signal Process. Image Commun.*, vol. 19, no. 3, pp. 257–265, Mar. 2004.

[17] J. Goutsias and H. J. A. M. Heijmans, "Nonlinear multiresolution signal decomposition schemes—Part I: Morphological pyramids," *IEEE Trans. Image Process.*, vol. 9, no. 11, pp. 1862–1876, Nov. 2000.

[18] H. J. A. M. Heijmans and J. Goutsias, "Nonlinear multiresolution signal decomposition schemes—Part II: Morphological wavelets," *IEEE Trans. Image Process.*, vol. 9, no. 11, pp. 1897–1913, Nov. 2000.

[19] Y. Zhang, J. Zhang, R. Xiong, D. Zhao, and S. Ma, "Low bit-rate image coding via interpolation oriented adaptive down-sampling," in *Proc. SPIE, Visual Commun. Image Process.*, Jul. 2010, p. 77 441C.

[20] *Spatial Scalability Filters*, ISO/IEC JTC1/SC29/WG11 and ITU-T SG16 Q.6, Jul. 2005.

Cellular Neural Networks, the Navier–Stokes Equation, and Microarray Image Reconstruction

Bachar Zineddin, Zidong Wang, and Xiaohui Liu

***Abstract*—Although the last decade has witnessed a great deal of improvements achieved for the microarray technology, many major developments in all the main stages of this technology, including image processing, are still needed. Some hardware implementations of microarray image processing have been proposed in the literature and proved to be promising alternatives to the currently available software systems. However, the main drawback of those proposed approaches is the unsuitable addressing of the quantification of the gene spot in a realistic way without any assumption about the image surface. Our aim in this paper is to present a new image-reconstruction algorithm using the cellular neural network that solves the Navier–Stokes equation. This algorithm offers a robust method for estimating the background signal within the gene-spot region. The MATCNN toolbox for Matlab is used to test the proposed method. Quantitative comparisons are carried out, i.e., in terms of objective criteria, between our approach and some other available methods. It is shown that the proposed algorithm gives highly accurate and realistic measurements in a fully automated manner within a remarkably efficient time.**

***Index Terms*—cDNA microarray reconstruction, cellular neural networks (CNN), isotropic diffusion, Navier–Stokes equations (NSEs), partial differential equations (PDEs).**

I. Introduction

DNA microarray is a remarkably successful high-throughput technology for functional genomics [23]. Microarrays allow researchers to collect quantitative data about the expression level of many thousands of genes in a single experiment. Therefore, it offers a deep understanding of gene interaction and regulation. However, the microarray

Manuscript received October 13, 2010; revised April 07, 2011; accepted May 24, 2011. Date of publication June 09, 2011; date of current version October 19, 2011. The associate editor coordinating the review of this manuscript and approving it for publication was Prof. Rafael Molina.

The authors are with the Department of Information Systems and Computing, Brunel University, Uxbridge UB8 3PH, U.K. (e-mail: bachar.zineddin@gmail.com; Zidong.Wang@brunel.ac.uk; Xiaohui.Liu@brunel.ac.uk).

Color versions of one or more of the figures in this paper are available online at http://ieeexplore.ieee.org.

Digital Object Identifier 10.1109/TIP.2011.2159231